Prepared Nd:YAG nano-particles by using co-precipitation process

Hung-Hua Sheu[1*], Sin-De Lin[1], Ming-Der Ger[1] and Li-Chuan Chen[2]

[1] Department of Chemical and Materials Engineering, Chung Cheng Institute Technology, National Defense University, Da-Xi, Tao-Yuan, Taiwan 335, ROC
[2] Materials & Electro-Optics Research Division, National Chung-Shan Institute of Science & Technology, Da-Xi, Tao-Yuan, Taiwan 335, ROC

Abstract

In this study, the 0.1 at.% Nd doped Nd:YAG nano-particles were successfully prepared using co-precipitation method under different concentration of precipitating agent and precipitation temperature. The Nd:YAG precursors obtained from co-precipitation process were calcined at different temperature. The XRD patterns revealed that the formation of YAM, YAP and YAG phase occurred at 800℃, and the quantity of YAP and YAM phases decreased with an increase of calcined temperature. The precursors transformed into a single YAG phase when the calcined temperature at 1200℃. The average particles size of Nd:YAG distributed between 150 to 280 nm, and it decreased with a decrease of co-precipitation temperature. The analysis of EPMA and ICP-OES showed the composition of Nd:YAG corresponded to the stoichiometric ratio of Y/Al about 0.6±0.06 and doped neodymium at 0.1 at.%. Finally, the results of Taguchi method presented the main factor affected the particles size and chemical composition of Nd:YAG during co-precipitation process was the concentration of precipitating agent.

Keywords: Nd:YAG powders, co-precipitation method, Taguchi method

利用共沉澱法製備 Nd:YAG 奈米粉末之研究

許宏華[1*]　林賜德[1]　葛明德[1]　陳麗娟[2]

[1] 國防大學理工學院化學與材料工程學系
[2] 國家中山科學研究院光學暨材料科學研究所

摘　要

本研究利用不同沉澱劑(NH_4HCO_3)濃度及沉澱溫度作為共沉澱製程的主要實驗參數，並成功地製備 Nd:YAG 奈米粉體。共沉澱製程所獲得的前驅體粉末，分別經過 800、900、1000、1100 及 1200℃煅燒後，並經過 X 光繞射檢測。XRD 結果顯示當前驅體粉末經過 800℃煅燒後開始形成 YAM、YAP 及 YAG 等相，隨著煅燒溫度增加，YAM 及 YAP 相的量會減少；當煅燒溫度升高至 1200℃時，粉體內部轉變為單一 YAG 相。經由 SEM 觀察後，發現 Nd:YAG 粉體的粒徑分布於 150-280 nm 之間，且粒徑分布隨著共沉澱溫度降低而減小；而成分分析(EPMA)結果顯示利用共沉積法所製備之 Nd:YAG 奈米粉體的化學計量符合 Y/Al=0.6±0.06。經過田口實驗分析法進行實驗控制因子之響應分析後，得知影響共沉積法製備 Nd:YAG 奈米粉體粒徑及成分計量比的主要因子均為沉澱劑濃度。

關鍵詞： Nd:YAG 粉末、共沉澱法、田口法

文稿收件日期 104.10.28;文稿修正後接受日期 105.03.02; *通訊作者
Manuscript received October 28, 2015; revised March 02, 2016; * Corresponding author

I. INTRODUCTION

Transparent yttrium aluminum garnet (YAG) based single crystal has an excellent optical property owing to its cubic form, garnet structure and no birefringence effect at the grain boundaries [1]. Rare earth ion doped YAG laser materials, such as Nd:YAG [2,3] have been studied widely and deeply for laser applications. However, it is difficult for such a single crystal to make a big size, high doping concentration and low production cost. Therefore, in recently two decades, the researchers studied a sintered polycrystalline YAG transparent ceramic that has a low production cost, excellent optical and good high temperature mechanical properties as compared to YAG single crystal [4,5].

In 1995, Ikesue et al. showed that the solid-state reaction method was possible to obtain a laser effect with a polycrystalline yttrium aluminium garnet doped with neodymium (Nd:YAG) [2]. In general, YAG powder was produced by solid-state reaction between aluminium and yttrium oxides. This method involved extensive heat treatment at high temperature (~1700 ℃) to eliminate secondary phases such as YAM ($Y_4Al_2O_9$) and YAP ($YAlO_3$). Furthermore, mechanical mixing and grinding leaded to possible contamination. However, the main disadvantage of this process is that the incorporation of some impurities is unavoidable during ball milling. Another disadvantage is it requires long time and very high temperature. In order to improve the disadvantages of solid-state reaction method, several techniques were developed such as solvothermal synthesis [6,7], sol–gel route [8,9], nitrate–citrate combustion [10,11] and co-precipitation method [12–14]. Among these approaches, co-precipitation is a relatively simple way to synthesize YAG powder with excellent chemical homogeneity, good crystallinity and pure phase at low temperature. Many studies have hence focused on synthesis of high purity and agglomeration-free powders [15–17]. However, the presence of agglomerates may inevitably inhibit homogeneous distribution of the powders and then affect the sinter-ability of powders. It is well known that optical property of Nd:YAG ceramic is closely related with the powders characteristics, including size distribution, particle shape, degree of agglomeration, chemical composition. Therefore, the dispersion of particles and the sinter-ability of Nd:YAG powders still remain as the most common concern for the co-precipitation method. Moreover, there are some important factors to affect the Y/Al chemical composition ratio such as dripping rate of precipitating agent, concentration of precipitating agent, co-precipitant temperature and stirring rate [14].

In this study, we focus on how to fabricated the highly quality Nd:YAG ceramics which has an average particles size about 180 nm and a homogeneous composition ratio of Y/Al ratio is about 0.6±0.06. Therefore, the Taguchi method was used to analyze the effects of experimental factors including concentration of precipitating agent, dripping rate, co-precipitation temperature and stirring rate. We systematically optimize the above experimental factors for fabrication of highly transparent Nd:YAG nano-particles during co-precipitation process. After an optimization of operated parameters, we can find that the concentration of precipitating agent was the main experimental factor to dominate the particles size and chemical composition of Nd:YAG nano-particles.

Ⅱ. EXPERIMENTAL

2.1 Materials：

In this study, yttrium nitrate hydrate ($Y(NO_3)_3 \cdot H_2O$, purity > 99.9%, Alfa Co. Ltd.), aluminum nitrate hydrate ($Al(NO_3)_3 \cdot H_2O$, purity > 99.9%, , Sigma-aldrich Co. Ltd.) , neodymium nitrate ($Nd(NO_3)_3 \cdot 6H_2O$, purity > 99.9%, Alfa Co. Ltd.) and ammonia bicarbonate (NH_4HCO_3, analytical reagent, purity > 99.9%, , Sigma-Aldrich Co. Ltd.) were used as raw materials. The starting solutions were made by dissolving the corresponding raw materials into deionized water following being filtered.

2.2 Fundamental of Taguchi method

Developed by Genichi Taguchi, Taguchi statistical method is widely known as a robust and powerful engineering tool for experimental optimization and design method [18]. This method is employed to assess sensitivity of each parameter and determine the optimum combination of the design factors. In this study,

four key parameters determining the performance of co-precipitant process are evaluated; those are concentration of precipitant, titration rate, co-precipitant temperature and stirring rate. Three values are evaluated for each parameter, as presented in Table 1. As such an L_9 orthogonal array is utilized in this computational evaluation as shown in Table 2.

Table1. Taguchi array design of four independent variables with three levels

Symbol	Factors	Level 1	Level 2	Level 3
A	concentration of precipitant (M)	1.0	1.5	2.0
B	dripping rate (ml/min)	15	20	30
C	co-precipitant temperature (℃)	0	10	25
D	stirring rate (rpm)	200	300	400

Table 2. L_9 array has been suggested by Taguchi method for 4 parameters at 3 levels

Experiment series	A	B	C	D
	Levels			
1	1	1	3	1
2	1	2	2	2
3	1	3	1	3
4	2	1	2	3
5	2	2	1	1
6	2	3	3	2
7	3	1	1	2
8	3	2	3	3
9	3	3	2	1

The Taguchi method uses an orthogonal array, consisting of factors and levels, to classify the experimental results. There are three basic categories to seek the best results of experiments; they are the nominal-the-better (NB), the larger-the-better (LB), and the smaller-the-better (SB) [18]. By introducing a parameter of signal-to-noise (S/N) ratio, the sensitivity of the parameters on the physical behavior can be figured out clearly. In this work, the suitable particles size of Nd:YAG powders, the NB criterion is thus adopted. The S/N ratio in terms of suitable particles size of Nd:YAG powders is written as

$$SN = 10 \log \left(\frac{\bar{y}^2}{s^2} \right) \tag{2.1}$$

where

$$\bar{y} = \frac{\sum_{i=1}^{n} y_i}{n} \tag{2.2}$$

$$s = \sqrt{\frac{\sum_{i=1}^{n} \left(y_i - \bar{y} \right)^2}{n-1}} \tag{2.3}$$

2.3 Co-precipitated process

$Y(NO_3)_3 \cdot 6H_2O$ and $Al(NO_3)_3 \cdot 9H_2O$ in the molar ratio of 3:5 were dissolved into the deionized water to obtain a mixed solution in which the concentration of both Y^{3+} and Al^{3+} was 0.5 mol/L. The composition of doped neodymium was kept at 0.1 at.%. The precipitating agent was prepared by dissolving ammonium hydrogen carbonate (NH_4HCO_3, analytical grade) in mixed solvent of alcohol and distilled water. The precipitating agent was dripped into the mixed solution at different dripping speed between 15 to 30 ml/min controlled by a peristaltic pump under stirring at different co-precipitant temperature (0, 10 and 25℃) . With the suspension aged for 48 h, filtered and washed with distilled water and alcohol, the precipitate was obtained. Then precursors were produced after the precipitate was dried at 90℃ for 72 h in a drier. The obtained precursors were sieved 200-mesh screen and then in air calcined at various temperatures from 800 to 1200℃ for 2 h to obtain pure Nd:YAG nano-powder.

2.4 Nd:YAG Powder characterization

Thermal gravimetric analysis and differential thermal analysis (TG–DTA) of the original precursor were recorded on a Netzsch STA 449C Instrument. Measurements were taken under a continuous flow of N_2 (20 ml/min). Samples were heated from room temperature to 1200 ℃ at 10 ℃/min and then cooled to room temperature naturally to determine the transformation temperature of YAG phase and the weight loss during reaction process.

The phase analysis was performed using diffractometer (XRD, Model D2 PHASER,

Bruker, Germany). The X-ray radiation source used was Cu K_α, obtained at 40 kV, 100 mA. The morphologies of Nd:YAG powders were observed using field emission scanning electron microscope (FESEM, Model JSM-6700F, JEOL, Japan). The average particles size of powder was estimated by statistically analyzing 25 sizes in the SEM images. The chemical composition of doped neodymium (0.1 at.%) was analyzed by an inductively coupled plasma optical emission spectrometer (ICP-OES, Agilent-725, USA).

Ⅲ. RESULTS and DISCUSSION

3.1 Thermal analysis

Fig. 1 shows the TG-DTA curves of the precursors precipitated at the same concentration of precipitating agent (1.5 M) and different co-precipitation temperature (0-5℃, 10-15℃ and room temperature), respectively. Fig. 1(a) shows the precursor precipitated at 0-5 ℃ has a weight loss about 55% when the temperature heated up to 750℃. Above 750℃, the weight loss of Nd:YAG precursor maintains a slightly change. The endothermic peak occurred at 150 ℃ is the contribution of moisture absorbed on the surface of sample, and there is a very sharp weight loss corresponding to the TG curve. The endothermic peak at 200℃ is attributed to the decomposition of carbonate and hydroxyl compounds [20]. Fig. 1(b) and (c) show the TG-DTA curves of the precursors precipitated at 10-15℃ and room temperature, respectively. The same endothermic peaks occur at the temperature between 150 and 200℃, which indicated the decomposition of moisture, carbonate and hydroxyl compounds, and they have weight loss about 52 and 54%, respectively. In this work, the weight loss of Nd:YAG was similar to paste literatures [12-14, 19, 20]. The exothermic peak occur at 900-1000 ℃ such as the red arrow marked in the Fig. 1 (a)-(c) should be the formation of YAG phase [19-21].

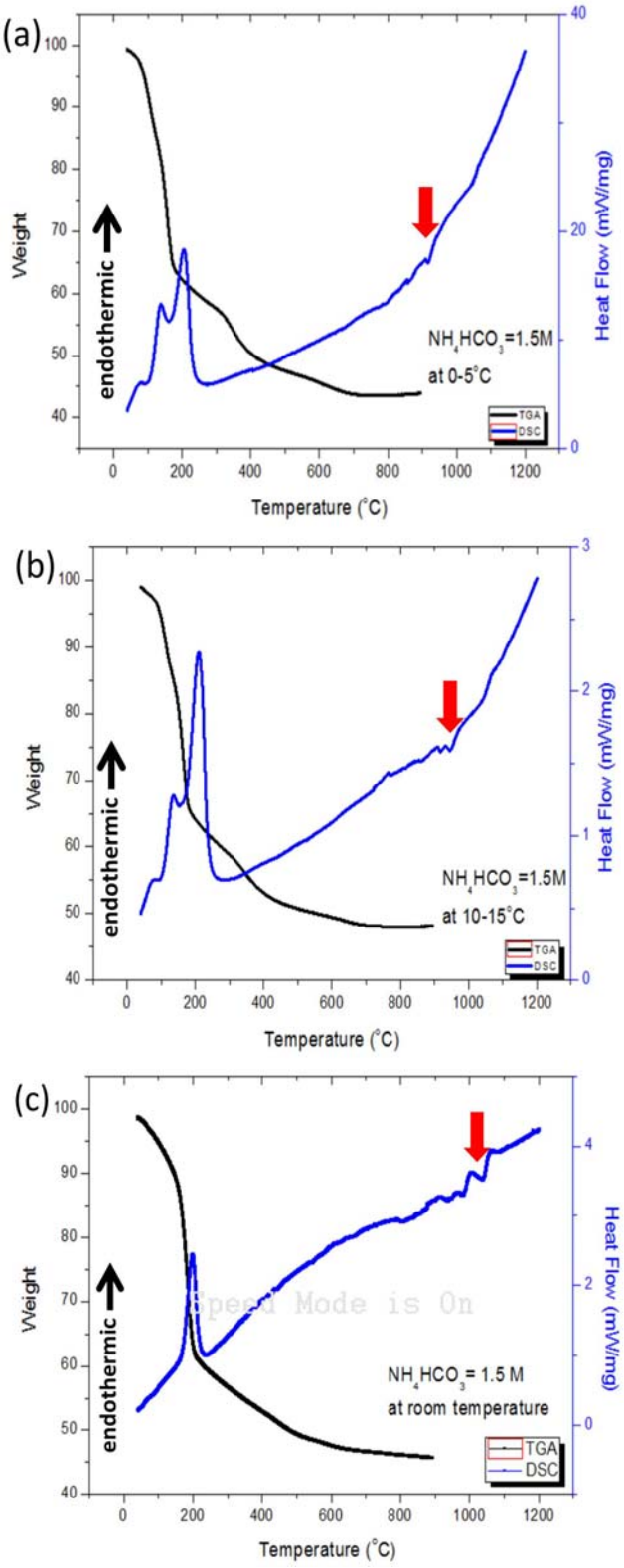

Fig. 1. DSC–TG curves of the Nd:YAG precursor samples precipitated at various temperature: (a) 0-5℃; (b) 10-15℃ and (c) 25℃.

3.2 XRD analysis

XRD patterns of the Nd:YAG powders (concentration of precipitant was 1.5 M) calcined at various temperatures for 2 h are shown in Fig. 2. Fig. 2(a) shows the XRD pattern of Nd:YAG precursors precipitated at various temperature, and they all present non-crystal structure in the precursors powders. Fig. 2(b) shows the XRD pattern of Nd:YAG precursors calcined at 800 ℃ and the characteristic diffraction peaks corresponded to the YAP phase ($YAlO_3$, JCPDS #16-219), respectively. Therefore, the exothermic peak occurred at 750℃ in TG-DTA curves should be the formation of YAP phase. Fig. 2(c) shows the XRD pattern of Nd:YAG precursors calcined at 900℃, the curves present several different phases formed within precursors such as YAP ($YAlO_3$), YAM ($Y_4Al_2O_9$, JCPDS #14-0475) and YAG ($Y_5Al_3O_{12}$, JCPDS #73-1370) phase. This indicated that intermediate phase (YAM phase) formed at 900℃ and the YAG phase also began form at the same temperature. Fig. 2(d) shows the XRD pattern of Nd:YAG precursors calcined at 1000℃, it revealed the diffraction intensity of YAM phase significantly decrease and this indicated the calcined temperature would play a dominated role in the formation of YAG phase. Therefore, we increased the concentration of precipitating agent and calcined temperature to 2 M and 1200 ℃, respectively. Fig. 3 shows the XRD pattern of Nd: YAG precursors precipitated at different temperature with the same concentration of precipitating agent (2M). By comparing with Fig. 2, it can observe the YAM phase almost disappear in the powders. The result indicated the higher temperature and concentration of precipitating agent will help the formation of YAG phase. In this work, the phase transformation of Nd:YAG precursor calcined from 800 to 1200℃ was similar to the study completed by X. Li et. al. [22].

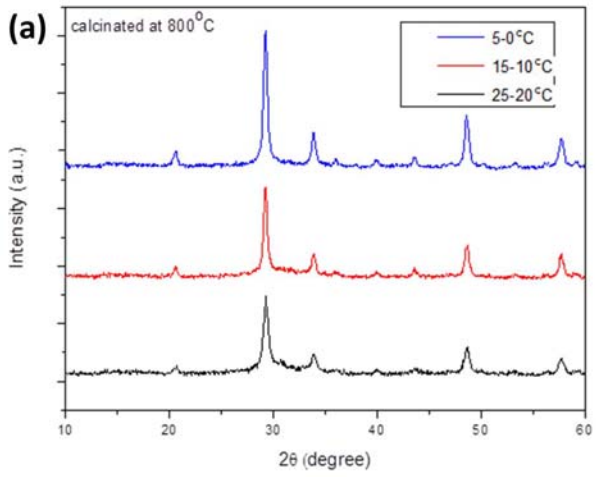

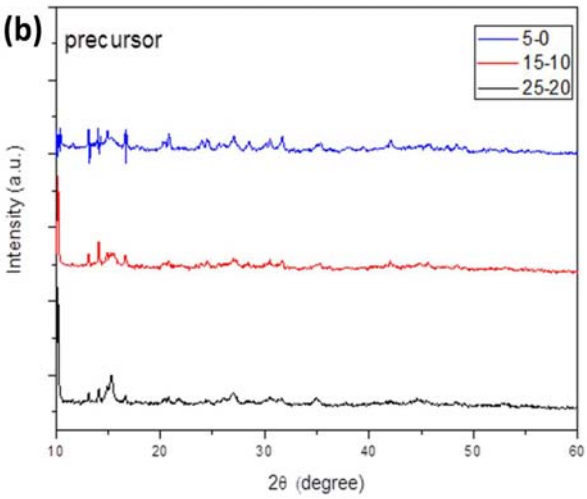

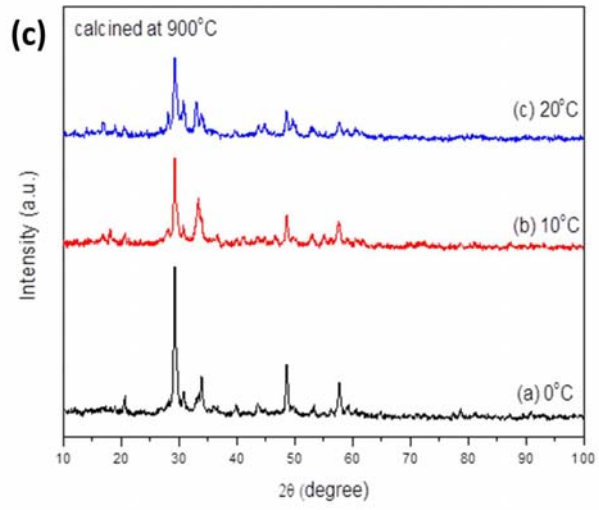

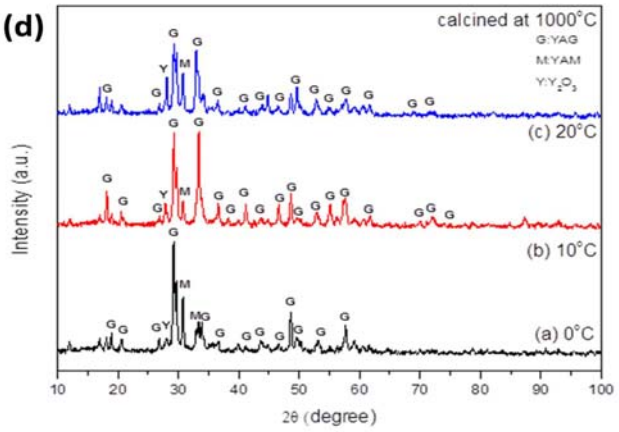

Fig. 2. XRD spectra of Nd:YAG nano-powders precipitated at various temperature and calcined temperature (a) precursor; (b) 800 ℃; (c)900 ℃ and (d) 1000 ℃.

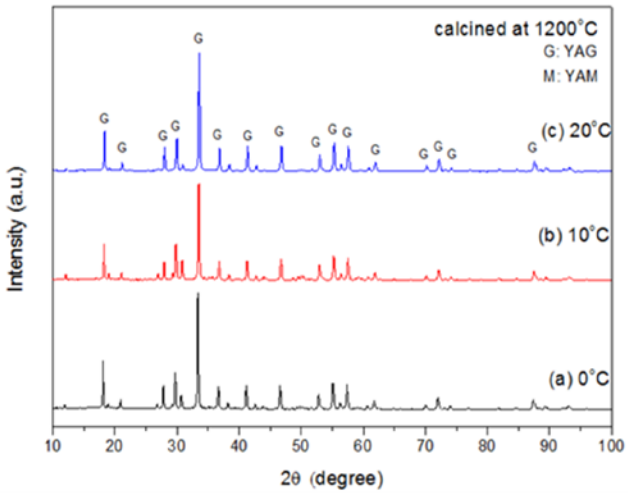

Fig. 3. XRD spectra of Nd:YAG precursor precipitated at various temperature and calcined at 1200℃ when the precipitating agent concentration was 2 M: (a) 0℃; (b) 10 ℃ and (c) 20℃.

3.3 SEM analysis of Nd:YAG precursors

Fig. 4 shows the SEM morphology images of Nd:YAG precursors precipitated at 0℃ and different precipitating agent concentration (1, 1.5 and 2 M). Fig. 4(a) shows the SEM image of Nd:YAG precursors co-precipitated at 1M NH_4HCO_3 and 0℃, it revealed the Nd:YAG precursor dispersed with an average particle sizes between 50-100 nm. When the concentration of precipitating agent increased to 1.5 M, the Nd:YAG precursors had a few agglomerations of several particles but still can be observed the dispersed particles (Fig. 4(b)). Fig. 4(c) shows the co-precipitation of Nd:YAG precursors at 2M NH_4HCO_3 , the precursors almost agglomerated as a bulk-like structure and the average size of bulk-like structure was between 700-1100 nm. This should be the higher concentration of precipitating agent will accelerate the chemical reaction within in the solutions and lead to the nucleation sites of YAG precursor concentrate excessively. Finally, the YAG precursor agglomerated as a bulk-like structure during the co-precipitation process.

Fig. 5 shows the SEM morphology images of Nd:YAG precursors precipitated at 10℃ and different precipitating agent concentration (1, 1.5 and 2 M). Fig. 5(a) shows the SEM image of Nd:YAG precursors precipitated at 1 M NH_4HCO_3 and 10℃, it also revealed the

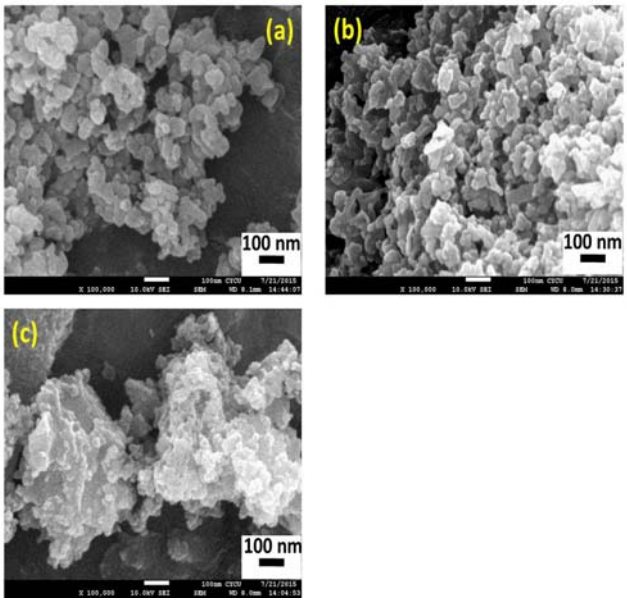

Fig. 4. SEM micrographs of the Nd:YAG precursor co-precipitated at 0 ℃ and various precipitating agent concentration: (a) 1 M; (b) 1.5 M and (c) 2 M.

Nd:YAG precursor was formed as a well dispersed fine grains and with an average particle sizes between 100-140 nm. When the precipitating agent concentration increased to 1.5 M, the particles of Nd:YAG precursors did not agglomerate and on the contrary it was formed as a well dispersed fine grains and with an average particle sizes between 40-70 nm. (Fig. 5(b)). Fig. 5(c) presents the co-precipitation of Nd:YAG precursors at 2 M NH_4HCO_3 and 10℃, by comparing with Fig.

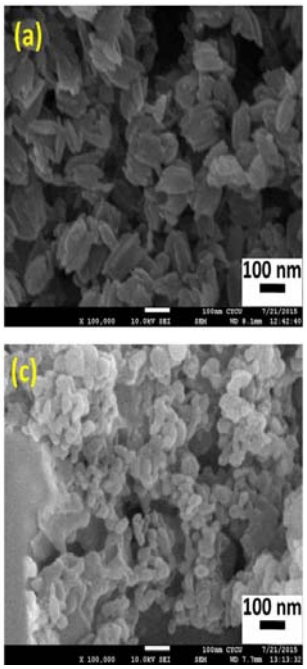

Fig. 5. SEM micrographs of the Nd:YAG precursor co-precipitated at 10 ℃ and various precipitating agent concentration: (a) 1 M; (b) 1.5 M and (c) 2 M.

4(c), the precursors still did not agglomerate together and the average particles size were distributed between 50-100 nm.

Fig. 6 presents the SEM images of Nd:YAG precursors co-precipitated at 20 ℃ and various precipitating agent concentration. When the precipitating agent concentration was at 1 M, the morphology of Nd:YAG precursors still retain a particle structure (Fig. 6(a)), but the Nd:YAG precursors will agglomerate together seriously with an increase of precipitating agent concentration (Fig. 6(a) and (b)). The higher co-precipitation temperature and precipitating agent concentration will increase the chemical reaction and lead to the agglomeration of Nd:YAG precursors during co-precipitation process.

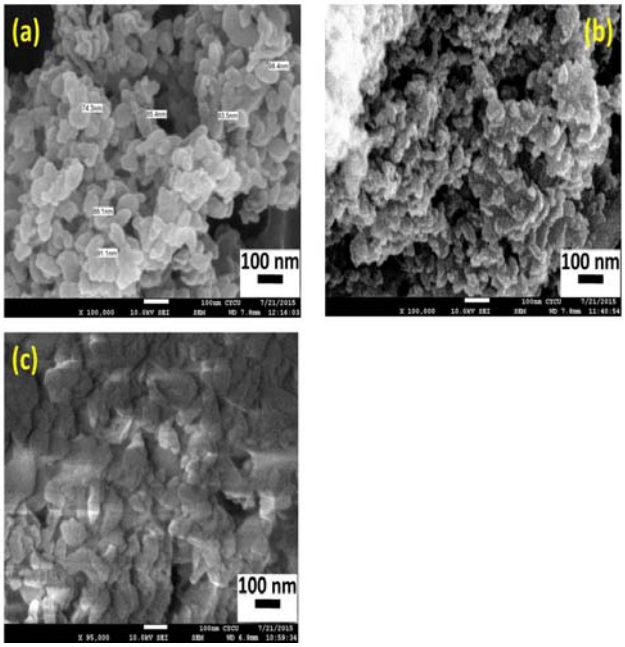

Fig. 6. SEM micrographs of the Nd:YAG precursor co-precipitated at 20 ℃ and various precipitating agent concentration: (a) 1 M; (b) 1.5 M and (c) 2 M.

3.4 SEM analysis of Nd:YAG precursors calcined at 1200℃

In Fig. 3, the XRD pattern indicated the high purity YAG phase was formed when the Nd:YAG precursors calcined at 1200 ℃. Therefore, all the Nd:YAG precursors co-precipitated at different conditions were calcined at 1200 ℃ and the particles morphology was observed by using SEM. Fig. 7 shows the SEM images of Nd:YAG precursors co-precipitated at various precipitating agent concentration under 10℃ and then calcined at 1200℃. Fig. 7(a) presents the average particles size of Nd:YAG nano-particles (precipitating agent concentration was 1 M) was about 165 nm. The average particles size of Nd:YAG at precipitating agent concentration 1.5 M was about 186 nm (Fig. 7(b)). The average particles size of Nd:YAG at precipitating agent concentration 2 M was about 279 nm (Fig. 7(c)). The experimental results revealed the particles size of Nd:YAG increased with an increase of precipitating agent concentration at the same co-precipitated temperature.

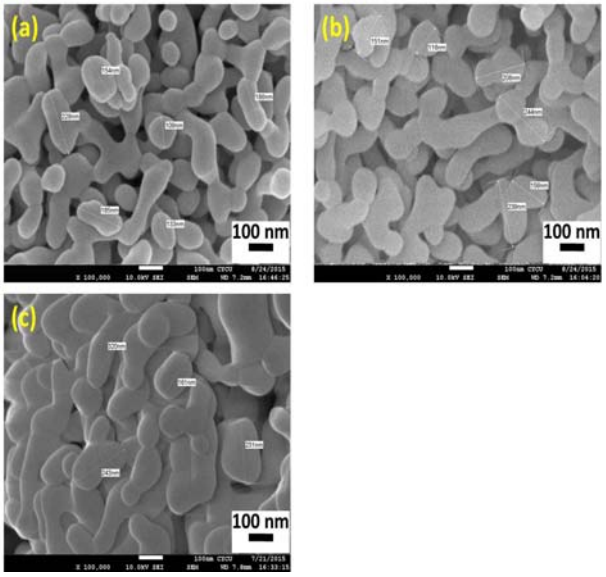

Fig. 7. SEM micrographs of the Nd:YAG precursor co-precipitated at 10 ℃, various precipitating agent concentration and calcined at 1200℃: (a) 1 M; (b) 1.5 M and (c) 2 M.

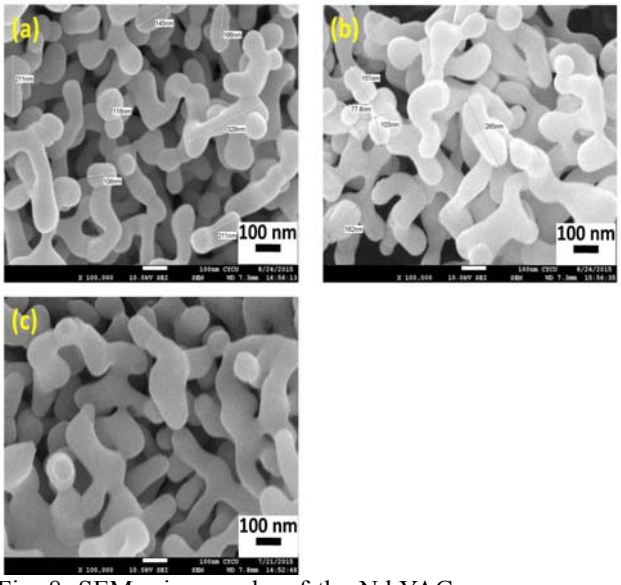

Fig. 8. SEM micrographs of the Nd:YAG precursor co-precipitated at 20 ℃, various precipitating agent concentration and calcined at 1200℃: (a) 1 M; (b) 1.5 M and (c) 2 M.

Fig. 8 shows the SEM images of Nd:YAG precursors co-precipitated at various precipitating agent concentration under 20℃ and then calcined at 1200℃. Fig. 8(a) presents the average particles size of Nd:YAG nano-particles (precipitating agent concentration was 1 M) was about 195 nm. The average particles size of Nd:YAG co-precipitated at precipitating agent concentration 1.5 M was about 239 nm (Fig. 8(b)). The average particles size of Nd:YAG co-precipitated at precipitating agent concentration 2 M was about 368 nm (Fig. 8(c)).

Fig. 9 shows the relationship between particles size of Nd:YAG precursors calcined at 1200℃ and precipitating agent concentration at different co-precipitated temperature. The curves indicated the Nd:YAG precursors co-precipitated at 0℃ and then calcined at 1200℃ has the smallest amount of particle size change. The Nd:YAG precursors co-precipitated at 20℃ and then calcined at 1200℃ has the largest amount of particle size change. Therefore, both co-precipitated temperature and precipitating agent concentration will dominate the particle size change of Nd:YAG nano-particles.

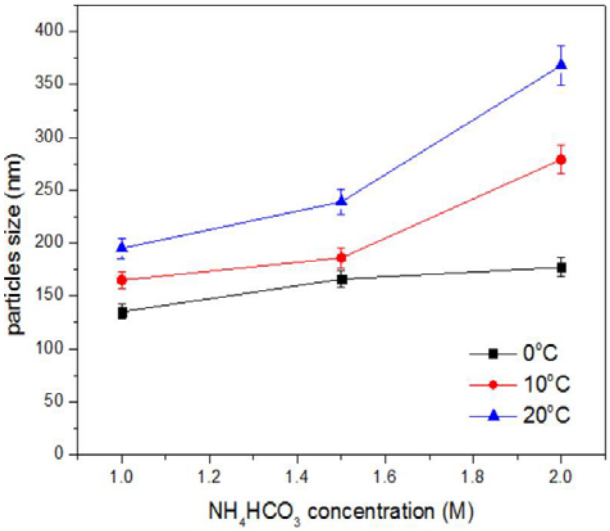

Fig 9. Relationship between particles size of Nd:YAG precursors calcined at 1200℃ and precipitating agent concentration at different co-precipitated temperature.

The effects of experimental factors (concentration of precipitant, dripping rate, co-precipitant temperature and stirring rate) on the particles size and chemical composition of Nd:YAG nano-particles were analyzed by using Taguchi method which was applied to calculate the S/N response for particles size and chemical composition of Nd:YAG nano-particle, respectively. Each experiment was run for three times and determined the average particles size. The analysis of particles size was calculated by

the nominal-the-better (NB) formula to obtain the S/N response data (Table 4). In this study, the expected average particles size was about 180 nm.

The delta values for individual factors were derived from the S/N ratio values and shown in Table 5. The highest difference was seen for the concentration of precipitant indicating its highest influence. In order to get the expected particles size, a high level of concentration of precipitant (2 M), low level of dripping rate (15 ml/min), low level of co-precipitant temperature (0℃) and middle level of stirring rate (300 rpm) are preferred.

Table 4. Results of experimental process carried out in L_9 orthogonal array.

Exp. Run	A	B	C	D	P1	P2	P3	$\bar{y}$	S/N
1	1	1	3	1	195	189	197	193.6	33.35
2	1	2	2	2	169	165	171	168.3	34.82
3	1	3	1	3	135	141	133	136.3	30.30
4	2	1	2	3	185	191	189	188.3	35.79
5	2	2	1	1	161	164	166	163.6	35.66
6	2	3	3	2	238	242	240	240	41.58
7	3	1	1	2	174	176	179	176.3	36.90
8	3	2	3	3	374	365	369	369.3	38.26
9	3	3	2	1	279	284	281	281.3	40.96

Table 5. S/N response for Nd:YAG particles size (the nominal-the-better)

Mean S/N ratio	Parameters			
	concentration of precipitant (M)	dripping rate (ml/min)	co-precipitant temperature (℃)	stirring rate (rpm)
1	32.82	35.34	34.28	36.65
2	37.67	36.24	37.19	37.76
3	38.70	37.61	37.73	34.78
Max-Min	5.88	2.27	3.45	2.98
Rank	1	4	2	3

3.5 EPMA analysis of Nd:YAG nano-particles

In order to analyze the chemical composition of Nd:YAG nano-particles at different experimental conditions, the EPMA analysis was carried out. Table 6 to 8 show the EPMA analysis of Nd:YAG nano-particles prepared at various temperature, concentration of precipitant and then calcined at 1200℃, respectively. From the Tables, the best chemical composition corresponded to the stoichiometric ratio of Y/Al equal to 0.6±0.06 occurred at concentration of precipitant at 2M and co-precipitated at 20℃. The main effect plot of each experimental factor to chemical composition of Nd:YAG nano-particles was shown in Fig. 10. The process parameters affecting the chemical composition of Nd:YAG nano-particles were in the following order: concentration of precipitant > dripping rate > co-precipitant temperature > stirring rate.

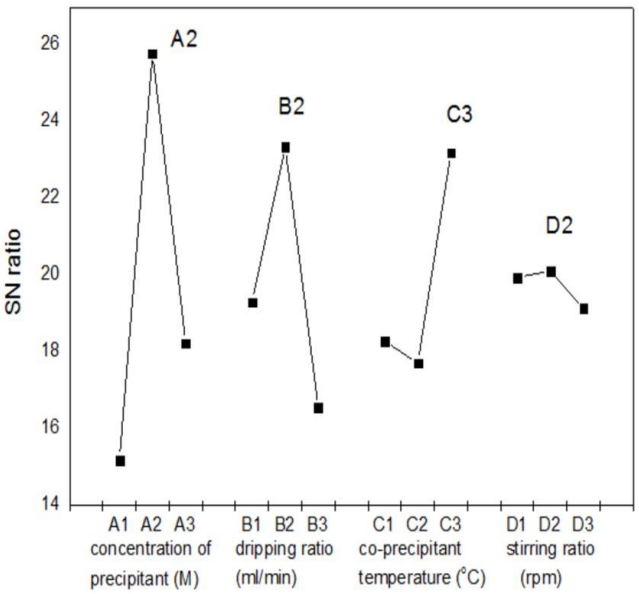

Fig. 10. Main effect plot for the chemical composition of Nd:YAG nano-particles.

Table 6. EPMA analysis of Nd:YAG nano-particles co-precipitated at various temperature (concentration of precipitant is 1M) and calcined at 1200℃

Analysis No.	Y (at. %)	Al (at. %)	Y：Al=3:5 (0.6±0.06)	Conditions
1	17.86	15.45	1.16	1.0M-20-1
2	11.26	23.53	0.48	1.0M-20-2
3	13.34	24.51	0.54	1.0M-20-3
4	13.01	21.36	0.61	1.0M-20-4
5	12.24	31.84	0.38	1.0M-20-5
6	6.95	30.92	0.23	1.0M-10-1
7	6.12	26.77	0.23	1.0M-10-2
8	7.63	25.44	0.3	1.0M-10-3
9	6.56	22.74	0.29	1.0M-10-4
10	5.75	26.89	0.21	1.0M-10-5
11	12.24	26.25	0.47	1.0M-0-1
12	15.60	19.13	0.82	1.0M-0-2
13	14.01	28.62	0.49	1.0M-0-3
14	10.75	22.07	0.49	1.0M-0-4
15	11.92	13.66	0.87	1.0M-0-5

Table 7. EPMA analysis of Nd:YAG nano-particles co-precipitated at various temperature (concentration of precipitant is 1.5M) and calcined at 1200℃

Analysis No.	Y (at. %)	Al (at. %)	Y：Al=3:5 (0.6±0.06)	Conditions
1	9.01	18.08	0.5	1.5M-20-1
2	13.10	28.64	0.46	1.5M-20-2
3	11.85	23.82	0.5	1.5M-20-3
4	9.07	27.49	0.33	1.5M-20-4
5	25.36	37.93	0.66	1.5M-20-5
6	15.78	15.92	0.99	1.5M-10-1
7	16.03	27.66	0.58	1.5M-10-2
8	13.25	19.41	0.66	1.5M-10-3
9	13.92	27.93	0.5	1.5M-10-4
10	15.01	22.62	0.66	1.5M-10-5
11	15.49	30.62	0.51	1.5M-0-1
12	14.61	26.55	0.55	1.5M-0-2
13	14.45	27.12	0.54	1.5M-0-3
14	13.39	22.19	0.6	1.5M-0-4
15	12.71	30.91	0.41	1.5M-0-5

Table 8. EPMA analysis of Nd:YAG nano-particles co-precipitated at various temperature (concentration of precipitant is 2M) and calcined at 1200℃

Analysis No.	Y (at. %)	Al (at. %)	Y：Al=3:5 (0.6±0.06)	Conditions
1	16.12	25.68	0.63	2M-20-1
2	24.78	34.40	0.71	2M-20-2
3	19.54	33.47	0.58	2M-20-3
4	24.15	36.79	0.62	2M-20-4
5	16.49	25.56	0.65	2M-20-5
6	15.09	22.83	0.66	2M-10-1
7	15.39	22.81	0.66	2M-10-2
8	20.83	20.29	1.03	2M-10-3
9	20.54	22.50	0.91	2M-10-4
10	22.41	18.32	1.22	2M-10-5
11	26.57	18.85	1.41	2M-0-1
12	16.77	19.44	0.86	2M-0-2
13	13.72	25.37	0.56	2M-0-3
14	14.24	21.50	0.66	2M-0-4
15	21.11	24.59	0.86	2M-0-5

3.6 ICP analysis of doped neodymium element

The chemical composition of doped neodymium was detected using inductively coupled plasma emission spectrometer (ICP-OES) and the experimental results were listed as Table 9. It can see the chemical composition of doped neodymium was remain at 0.1±0.02 at.%, indicated the Nd:YAG in this study corresponded to 0.1 at.% neodymium doped.

Table 9. The chemical composition of doped neodymium analyzed under various conditions using ICP-OES

conditions	doped neodymium (at. %)
1.0M-0	0.11
1.0M-10	0.12
1.0M-20	0.11
1.5M-0	0.12
1.5M-10	0.11
1.5M-20	0.10
2M-0	0.11
2M-10	0.12
2M-20	0.12

Ⅵ. CONCLUSIONS

The following main conclusions can be drawn from the results of this study.

1. Taguchi L_9 orthogonal array was used in this study for both the particles size and chemical composition of Nd:YAG particles during co-precipitated process. The most influential process parameters in particles size and chemical composition were concentration of precipitant.
2. Optimum parameters levels for expected average particles size at 180 nm were as A3B1C1D2.
3. In chemical composition of the stoichiometric ratio of Y/Al within Nd:YAG particles equal to 0.6±0.06, the most influential process parameter was concentration of precipitant. The process parameters affecting the chemical composition of Nd:YAG nano-particles were in the following order: concentration of precipitant > dripping rate > co-precipitant temperature > stirring rate.

V. REFERENCE

[1] Uehara, N. and Ueda, K., “Ultra-stabilized by laser diode pumped Nd:YAG lasers,” Rev. Lasers Eng., Vol. 21, pp. 590–600, 1993.

[2] Ikesue, A., Kinoshita, T., Kamata, K., and Yoshida, K., “Fabrication and Optical Properties of High-Performance Polycrystalline Nd:YAG Ceramics for Solid-State Lasers,” J. Am. Ceram. Soc., Vol. 78, pp. 1033–1040, 1995.

[3] Lu, J., Prabhu, M., Song, J., Li, C., Xu, J., Ueda, K., Kaminskii, A. A., Yagi, H., and Yanagitani, T., “Optical properties and highly efficient laser oscillation of Nd:YAG ceramics,” Appl. Phys. B., Vol. 71, pp. 469–473, 2000.

[4] With De, G. and Van Dijk, H. J. A., "Translucent $Y_3Al_5O_{12}$ ceramics," Mater. Res. Bull., Vol. 19, pp. 1669–1674, 1984.
[5] Sekita, M., Haneda, H., Yanagitani, T., and Shirasaki, S., "Induced emission cross section of Nd:$Y_3Al_5O_{12}$ ceramics," J. Appl. Phys., Vol. 67, pp. 453–458, 1990.
[6] Inoue, M., Otsu, H., Kominami, H., and Inui, T., "Synthesis of yttrium-aluminum-garnet by the glycothermal method," J. Am. Ceram. Soc., Vol. 74, pp. 1452–1454, 1991.
[7] Li, X., Liu, H., Wang, J. Y., Cui, H. M., Han, F., Zhang, X. D., and Boughton, R. I., "Rapid synthesis of YAG nano-sized powders by a novel method," Mater. Lett., Vol. 58, pp. 2377–2380, 2004.
[8] Gowda, G., "Synthesis of yttrium aluminates by the sol-gel process," J. Mater. Sci. Lett., Vol. 5, pp. 1029–1032, 1986.
[9] Yang, L., Lu, T. C., Xu, H., and Wei, N., "Synthesis of YAG powder by the modified sol–gel combustion method," J. Alloys Comp., Vol. 484, pp. 449–451 2009.
[10] Zhang, J. J., Ning, J. W., Liu, X. J., Pan, Y. B., Huang, L. P., Mater. Res. Bull., Vol. 38 pp. 1249–1256, 2003.
[11] Roy, S., Wang, L.W., Sigmund, W., and Aldinger, F., "Synthesis of YAG phase by a citrate-nitrate combustion technique," Mater. Lett., Vol. 39, pp. 138–141, 1999.
[12] Li, J., Chen, F., Liu, W. B., Zhang, W. X., Wang, L., and Ba, X. W., "Co-precipitation synthesis route to yttrium aluminum garnet (YAG) transparent ceramics," J. Eur. Ceram. Soc., Vol. 32, pp. 2971–2979, 2012.
[13] Yanagitani, T., Yagi, H., Ichikawa, M., "Production of yttrium aluminum garnet fine powder," JP patent 10-101333.
[14] Yanagitani, T., Yagi, H., Hiro, Y., "Production of fine powder of yttrium aluminum garnet," JP patent 10-101411.
[15] Tong, S., Lu, T., Guo, W., "Synthesis of YAG Powder by Alcohol-water Co-precipitation Method," Mater. Lett., Vol. 61, pp. 4287–4289 2007.
[16] Chen, Z. H., Yang, Y., Hu, Z. G., Li, J. T., and He, S. L., "Synthesis of highly sinterable YAG nano-powders by a modified co-precipitation method," J. Alloys Comp., Vol. 433, pp. 328–331, 2007.
[17] Deineka, T. G., Doroshenko, A. G., Mateychenko, P. V., Tolmachev, A. V., Vovk, E. A., Vovk, O. M., Yavetskiy, R. P., Baumer,V. N., and Sofronov, D. S., "Influence of sulfate ions on properties of co-precipitated $Y_3Al_5O_{12}:Nd^{3+}$ nano-powders," J. Alloys Comp., Vol. 508, pp. 200–205, 2010.
[18] Taguchi, G., Introduction to Quality Engineering, McGraw-Hill, New York, USA,
1990.
[19] Wang, L., Kou, H., Zeng, Y., Li, J., Pan, Y., and Guo, J., "Preparation of YAG powders and ceramics through mixed precipitation method," Ceramics International, Vol. 38, pp. 4401–4405, 2012.
[20] You, Y., Qin, L., Li, X., and Pan, W., "Preparation of YAG nano-powders via an ultra sonic spray co-precipitation method," Ceramics International, Vol. 39, pp. 3987–3992, 2013.
[21] Chen, X., Lu, T., Wei, Nian., Lu, Z., Chen, L., Zhang, Q., Cheng, G., and Qi, J., "Systematic optimization of ball milling for highly transparent Yb:YAG ceramic using co-precipitated raw powders," J. Alloys Comp., Vol. 653, pp. 552–560, 2015.
[22] Li, X., Zheng, B., Odoom-Wubah, T., and Huang, J., "Co-precipitation synthesis and two-step sintering of YAG powders for transparent ceramics," Ceramics International, Vol. 39, pp. 7983–7988, 2013.

Acknowledgements

The authors would like to thank the Ministry of Science and Technology of the Republic of China, Taiwan, for financially supporting this research under Contract No. MOST-104-2623-E-606 -002 –D.